

# Cardiotrophin-1 stimulates lipolysis through the regulation of main adipose tissue lipases<sup>S</sup>

Miguel López-Yoldi,<sup>\*,†</sup> Marta Fernández-Galilea,<sup>\*</sup> Laura M. Laiglesia,<sup>\*,†</sup> Eduardo Larequi,<sup>§</sup> Jesús Prieto,<sup>§,\*\*\*</sup> J. Alfredo Martínez,<sup>\*,†,††</sup> Matilde Bustos,<sup>1,§</sup> and Maria J. Moreno-Aliaga<sup>1,2,\*,†,††</sup>

Departments of Nutrition, Food Science, and Physiology\* and Gene Therapy and Hepatology, CIMA,<sup>§</sup> and Centre for Nutrition Research,<sup>†</sup> University of Navarra, Pamplona, Navarra, Spain; and CIBERehd<sup>\*\*</sup> and CIBERobn, Physiopathology of Obesity and Nutrition,<sup>††</sup> Institute of Health Carlos III, Madrid, Spain

**Abstract** Cardiotrophin-1 (CT-1) is a cytokine with antiobesity properties and with a role in lipid metabolism regulation and adipose tissue function. The aim of this study was to analyze the molecular mechanisms involved in the lipolytic actions of CT-1 in adipocytes. Recombinant CT-1 (rCT-1) effects on the main proteins and signaling pathways involved in the regulation of lipolysis were evaluated in 3T3-L1 adipocytes and in mice. rCT-1 treatment stimulated basal glycerol release in a concentration- and time-dependent manner in 3T3-L1 adipocytes. rCT-1 (20 ng/ml for 24 h) raised cAMP levels, and in parallel increased protein kinase (PK)A-mediated phosphorylation of perilipin and hormone sensitive lipase (HSL) at Ser660. siRNA knock-down of HSL or PKA, as well as pretreatment with the PKA inhibitor H89, blunted the CT-1-induced lipolysis, suggesting that the lipolytic action of CT-1 in adipocytes is mainly mediated by activation of HSL through the PKA pathway. In *ob/ob* mice, acute rCT-1 treatment also promoted PKA-mediated phosphorylation of perilipin and HSL at Ser660 and Ser563, and increased adipose triglyceride lipase (desnutrin) content in adipose tissue. These results showed that the ability of CT-1 to regulate the activity of the main lipases underlies the lipolytic action of this cytokine *in vitro* and *in vivo*, and could contribute to CT-1 antiobesity effects.—López-Yoldi, M., M. Fernández-Galilea, L. M. Laiglesia, E. Larequi, J. Prieto, J. A. Martínez, M. Bustos, and M. J. Moreno-Aliaga. **Cardiotrophin-1 stimulates lipolysis through the regulation of main adipose tissue lipases.** *J. Lipid Res.* 2014. 55: 2634–2643.

**Supplementary key words** adipocytes • adipose triglyceride lipase • cell signaling • cytokines • hormone-sensitive lipase • obesity • perilipin • protein kinase A

Cardiotrophin-1 (CT-1) belongs to the interleukin (IL)-6 family of cytokines. These cytokines exert their cellular

*This study was supported by grants from the Government of Navarra (Department of Health); Mutua Madrileña Foundation; FIS (PI10/01516 and PI13/01851); Línea Especial "Nutrición, Obesidad y Salud Universidad de Navarra"; and by the agreement between FIMA and the "UTE project CIMA". M.L.-Y. was supported by a doctoral grant from Asociación de Amigos University of Navarra.*

Manuscript received 3 October 2014.

Published, JLR Papers in Press, October 28, 2014  
DOI 10.1194/jlr.M055335

effects by interacting with the glycoprotein 130 (gp130)/leukemia inhibitory factor receptor heterodimer (1). Adipose tissue has been identified as a source of CT-1 (2), and this cytokine is capable of activating major signaling pathways involved in metabolic control in adipocytes (3). Moreover, it has been reported that CT-1 levels are raised in obesity and metabolic syndrome (2), suggesting that CT-1 could be a new marker for obesity and related diseases. A recent study by our group has revealed that CT-1 is a key regulator of energy homeostasis, as well as of glucose and lipid metabolism (4). Thus, chronic recombinant CT-1 (rCT-1) treatment reduced body weight and corrected insulin resistance in *ob/ob* and high-fat-fed obese mice by reducing food intake and enhancing energy expenditure. Moreover, rCT-1 induced dramatic white adipose tissue remodeling characterized by the upregulation of genes implicated in the control of fatty acid oxidation, mitochondrial biogenesis, and lipolysis. In this context, it has been reported that adipocytes from rCT-1-treated mice exhibited an increased lipolytic response to isoproterenol, while adipocytes from old obese CT-1-null mice responded poorly to isoproterenol, suggesting that CT-1 might play a role in the regulation of lipolysis (4). However, the mechanism underlying the lipolytic action of CT-1 still remains unknown.

During lipolysis, intracellular triacylglycerol (TAG) is hydrolyzed through the consecutive action of three major lipases: adipose triglyceride lipase (ATGL/desnutrin),

Abbreviations: AdPLA, adipocyte phospholipase A2; AICAR, aminoimidazole carboxamide ribonucleotide; ATGL, adipose triglyceride lipase (desnutrin); CGI-58, comparative gene identification-58; cGMP, cyclic guanosine monophosphate; CT-1, cardiotrophin-1; DAG, diacylglycerol; Gi, inhibitory guanine nucleotide binding protein; gp130, glycoprotein 130; Gs, stimulatory guanine nucleotide binding protein; G0S2, G0/G1 switch gene 2; HPTLC, high-performance TLC; HSL, hormone sensitive lipase; IL, interleukin; MAG, monoacylglycerol; PDE3B, phosphodiesterase 3B; PK, protein kinase; rCT-1, recombinant cardiotrophin-1; TAG, triacylglycerol.

<sup>1</sup>M. Bustos and M. J. Moreno-Aliaga contributed equally to the work.

<sup>2</sup>To whom correspondence should be addressed.

e-mail: mjmoreno@unav.es

<sup>S</sup>The online version of this article (available at <http://www.jlr.org>) contains supplementary data in the form of three figures.

hormone sensitive lipase (HSL), and monoacylglycerol (MAG) lipase. ATGL exhibits higher substrate specificity for TAG than diacylglycerol (DAG), and selectively assumes the first step in TAG hydrolysis resulting in the formation of DAG and fatty acid (5). ATGL lipolytic activity is coactivated by the protein comparative gene identification-58 (CGI-58), whereas it is inhibited by the protein G0/G1 switch gene 2 (G0S2) (6, 7). Moreover, recent findings describe how ATGL can also be regulated through phosphorylation by AMPK at Ser406, stimulating its lipolytic activity (8).

It is well-known that the activity of HSL is controlled postranscriptionally through reversible phosphorylation. Experiments in murine adipocytes have demonstrated that Ser563, Ser659, and Ser660 are the major protein kinase (PKA) phosphorylation sites, which are essential for the translocation of HSL to the lipid droplet surface and for stimulation of HSL (9). Besides PKA phosphorylation, HSL can also be phosphorylated by other kinases, such as ERK, which phosphorylates HSL at Ser600, increasing lipolysis (10). Another serine residue (Ser565) is a substrate of AMPK, which phosphorylates HSL preventing PKA-mediated activation of HSL by phosphorylation (11).

Perilipin A is a protein associated with the cytoplasm side of the lipid droplets (12). Under basal conditions, perilipin A maintains a low rate of basal lipolysis by sequestering CGI-58 (13) and by restricting the access of cytosolic lipases to the lipid droplet. However, cAMP-mediated activation of PKA induces conformational changes in perilipin A, facilitating the translocation of phosphorylated HSL from the cytoplasm to the lipid droplet surface and enhancing the lipolytic process (14).

Based on these previous findings, we aimed at analyzing whether the lipolytic actions of rCT-1 in adipocytes are mediated by changes in the regulation of the major lipases and lipid droplet proteins involved in the hydrolysis of TAG, and to characterize the major signaling pathways implicated.

## MATERIALS AND METHODS

### Cell culture and differentiation of 3T3-L1 cells

Mouse embryo fibroblast 3T3-L1 cells (American Type Culture Collection, Rockville, MD) were cultured in DMEM containing 25 mM glucose, 10% (v/v) calf bovine serum (Invitrogen, Carlsbad, CA), and 1% (v/v) penicillin/streptomycin (Invitrogen), and maintained in an incubator set to 37°C and 5% of carbon dioxide. At confluence, preadipocytes were cultured for 48 h in DMEM (Invitrogen) containing 25 mM glucose, 10% FBS (Invitrogen), and antibiotics, and supplemented with dexamethasone (1 mM; Sigma, St. Louis, MO), isobutylmethylxanthine (0.5 mM; Sigma), and insulin (10 µg/ml; Sigma). After that, cells were cultured with 10% FBS and insulin for 48 h and then media were replaced with 10% FBS in DMEM and antibiotics, but without insulin, and these media were changed every 2 days until day 8 postconfluence, when cells attained the morphology and typical features of mature adipocytes (15).

### rCT-1

rCT-1 was obtained as described elsewhere (16) and contained <0.04 ng LPS per 1 µg of the protein as determined by the Limulus amoebocyte lysate assay (Cambrex, East Rutherford, NJ).

### In vitro treatments

The inhibitors H89 (Santa Cruz Biotechnology, Santa Cruz, CA) and KT5823 (Calbiochem, La Jolla, CA) were dissolved in DMSO. The AMPK activator, aminoimidazole carboxamide ribonucleotide (AICAR) (Sigma), was dissolved in ultra-purified water. All compounds were prepared as 1,000× stock solutions and added to the culture medium. Control cells were treated with the same amount of vehicle (DMSO and/or ethanol).

Prior to the addition of the appropriate treatments, cells were serum starved for 4 h using the medium DMEM supplemented with 0.1% FBS and then treated with or without rCT-1 (1–40 ng/ml) during different time intervals (1–24 h). To analyze the signaling pathways involved in the lipolytic actions of rCT-1, adipocytes were preincubated for 1 h in presence or absence of specific inhibitors or activators (1 µM of PKA inhibitor H89, 2 mM of AMPK activator AICAR, and 1 µM of PKG inhibitor KT5823) before the addition of rCT-1 to the treated wells, as described elsewhere (15).

### Animal experiments

Eight-week-old male *ob/ob* (C57BL/6J background) mice were supplied by the Janvier Laboratory (Le Genest St. Isle, France). rCT-1 (0.2 mg/kg of body weight) was administered intravenously (retro-orbital injection) and animals were euthanized 30 min after administration. Control mice were injected with vehicle (saline). At the indicated time point, mice were euthanized and epididymal fat was snap-frozen in liquid nitrogen and stored at –80°C for subsequent analysis. All experimental procedures were performed according to the institutional guidelines for the use of laboratory animals and approved by the University of Navarra Ethics Committee.

### Determination of lipolysis in 3T3-L1 adipocytes

Lipolysis was evaluated by the biochemical determination of the amount of glycerol and FFAs released into the culture media. Glycerol measurements were performed after 1, 2, 12, 18, and 24 h of rCT-1 treatment using the Pentra C200 autoanalyzer (Roche Diagnostic, Basel, Switzerland), following manufacturer's instructions. FFAs were evaluated after 3 h of rCT-1 treatment by using a lipolysis assay kit for FFAs detection (Zen-Bio Inc., Research Triangle Park, NC) according to the manufacturer's instructions. TAG, DAG, and MAG levels were also determined by TLC. Briefly, cell lysates were mixed with an equal amount of chloroform/methanol (2:1; v/v). After vortexing for 1 min and resting for 10 min, the samples were centrifuged for 10 min. Organic layers were collected and vacuum dried. The pellets resolved in 40 µl chloroform/methanol (1:1, v/v) were applied as 5 mm spots to high-performance TLC (HPTLC)-silica gel with an aluminum backing (Merck, Darmstadt, Germany). The HPTLC plates were developed with a solvent system (hexane:diethyl ether:acetic acid, 70:30:1, v/v/v) at room temperature. The plate was dried and placed in a system with iodine salt vapor (Panreac, Barcelona, Spain) until the lipids were visible. Identities of the stained lipids were determined by referring to standards. Bands corresponding to TAG, DAG, and MAG were scraped from the plate and quantified using the ABX Pentra triglyceride CP (Horiba, Montpellier, France). For the determination of free cholesterol, the pellets were resolved using isopropanol, and free cholesterol was determined by the Wako Free Cholesterol E test (Wako, Neuss, Germany) (17).

## Ex vivo lipolysis assay in epididymal adipose tissue explants

Epididymal fat pads were surgically removed from overnight-fasted mice treated with either rCT-1 (0.2 mg/kg of body weight) or vehicle for 30 min. Fat pads of approximately 100 mg were minced into small pieces and incubated in 6-well plates with 1 ml of HEPES phosphate buffer (pH 7.4) (containing 5 mM D-glucose, 2% BSA, 135 mM NaCl, 2.2 mM  $\text{CaCl}_2 \cdot 2\text{H}_2\text{O}$ , 1.25 mM  $\text{MgSO}_4 \cdot 7\text{H}_2\text{O}$ , 0.45 mM  $\text{KH}_2\text{PO}_4$ , 2.17 mM  $\text{Na}_2\text{HPO}_4$ , and 10 mM HEPES) at 37°C. Media samples were collected at 1 h and 2 h of incubation. Glycerol content was quantified as described above and normalized by protein content.

## Determination of FFAs in serum samples

Serum FFAs were measured in mice fasted for 16 h, before and after 30 min treatment with vehicle or rCT-1 (0.2 mg/kg of body weight). FFAs were quantified using a Pentra C200 autoanalyzer (Roche Diagnostic, Basel, Switzerland), following manufacturer's instructions.

## Western blot analysis

3T3-L1 cell lysates were obtained by the addition of a buffer containing 2 mM Tris HCl (pH 8), 137 mM NaCl, 2 mM EDTA, 1% protease inhibitor cocktail 1 (Sigma), 2 mM orthovanadate, and 1 mM PMSF. In *ob/ob* mice, tissue samples were thawed and homogenized in lysis buffer [50 mM HEPES (pH 7.4), 1% Triton X-100, 0.1 M sodium fluoride, 10 mM EDTA, 50 mM sodium chloride, 10 mM orthovanadate, 0.1% SDS, and protease inhibitor cocktail (Roche)]. In both cases, samples were centrifuged and protein concentrations were determined by the BCA method according to the supplier's instructions (Pierce-Thermo Scientific, Rockford, IL). Briefly, equivalent amounts of total protein (25–50  $\mu\text{g}$ ) were electrophoretically separated by 12–15% SDS-PAGE in the presence of a reducing agent (2-mercaptoethanol). Proteins were electroblotted from the gel to polyvinylidene difluoride membranes (GE Healthcare Europe GmbH, Barcelona, Spain). Following the transfer of proteins, the membranes were blocked and probed with specific primary antibodies against phospho-HSL (Ser563), phospho-HSL (Ser565), phospho-HSL (Ser660), ATGL, phospho (Ser/Thr) PKA substrate, perlipin (Cell Signaling Technologies, Danvers, MA), G protein  $\alpha$  S ( $G_{\alpha}$ ), G protein  $\alpha$  inhibitor 1+2 (Gi) (Abcam, Cambridge, UK), phosphodiesterase 3B (PDE3B) (Phospho) (Acris Antibodies, Herford, Germany), adipocyte phospholipase A2 (AdPLA) (Cayman Chemical, Ann Arbor, MI), and  $\beta$ -actin (Sigma). After that, membranes were hybridized with horseradish peroxidase-conjugated secondary antibody (Sigma) for 1 h and then were revealed with the SuperSignal kit revelation solution (Pierce Biotechnology, Rockford, IL) following the manufacturer's protocol. The results were analyzed by densitometry using the GS-800 calibrated densitometer (Bio-Rad, München, Germany).

## cAMP assay

The cAMP Direct EIA kit (Arbor Assay, Ann Arbor, MI) was used to quantify the amount of intracellular cAMP after 24 h of control or rCT-1 treatment (20 ng/ml) in 3T3-L1 adipocytes.

## siRNA experiments

The predesigned siRNA specific to PKA (Silencer Select siRNA) and control siRNA (Silencer Select Control siRNA) were purchased from Ambion (Ambion Inc., Austin, TX), and siRNA specific to HSL and control were obtained from Santa Cruz. Transfection of 3T3-L1 adipocytes was performed using the

Amaxa® Cell Line Nucleofector® kit L with the Nucleofector® II system (Lonza, Basel, Switzerland) using the recommended settings according to the manufacturer's protocol. The transfected cells were seeded in 6-well plates, and experiments were conducted after 24 h incubation.

## Analyses of mRNA levels

Total RNA was extracted with TRIzol (Invitrogen) and real-time PCR was performed using iCycler (Bio-Rad) and iQ SYBR Green Supermix (Bio-Rad). For relative quantitation of gene expression, we used the comparative Ct method [ $2^{-\Delta\text{Ct}}$ , where  $\Delta\text{Ct}$  represents the difference in threshold cycle between the target and control genes (cyclophilin)]. Primers were designed according to published cDNA or genomic sequences.

## Statistical analysis

Data are presented as mean  $\pm$  SEM. Comparisons between the values for different variables were analyzed by one-way ANOVA followed by Bonferroni post hoc tests or by Student's *t*-tests or Mann-Whitney U-tests once the normality had been screened using Kolmogorov-Smirnoff and Shapiro-Wilk tests. Statistical analyses and graphs were carried out using GraphPad Prism 5 software (Graph-Pad Software Inc., San Diego, CA). Overall, a *P* value  $< 0.05$  was considered significant.

## RESULTS

### Effects of rCT-1 on lipolysis in 3T3-L1 adipocytes

The incubation with rCT-1 (1–20 ng/ml) significantly increased basal glycerol released to the media in a dose-dependent manner after 18 h of treatment. Similar effects on glycerol release were observed for IL-6 (Fig. 1A). Furthermore, the effect of rCT-1 (20 ng/ml) on lipolysis was time-dependent. As shown in Fig. 1B, a significant increase in glycerol release was seen in the rCT-1-treated group after 12 h ( $P < 0.01$ ) of incubation onwards, and this increase continued for up to at least 24 h ( $P < 0.001$ ). However, after 3 h treatment, a significant concentration-dependent increase in the amount of FFAs released was already observed in rCT-1-treated adipocytes ( $P < 0.05$ ) (Fig. 1C). Moreover, we also measured the intermediary metabolites after total lipid separation by HPTLC. Our data revealed that rCT-1 treatment did not induce any significant change in DAG and MAG levels, suggesting that the major products of rCT-1-induced TAG hydrolysis are FFAs and glycerol. Finally, because it has been described that in some tissues HSL also has lipolytic activity against cholesteryl esters (18), intracellular free cholesterol levels were tested. However, rCT-1-treated adipocytes showed no changes in intracellular free cholesterol (supplementary Fig. 1).

### Effects of rCT-1 on the main proteins involved in lipolysis control

For a better understanding of the mechanisms involved in CT-1 lipolytic actions, we first tested in 3T3-L1 adipocytes the effects of rCT-1 on ATGL, the enzyme that predominantly catalyzes the initial step in TAG hydrolysis (5). rCT-1 treatment for 1 and 2 h did not modify ATGL levels, but at 24 h the adipocytes treated with the cytokine exhibited



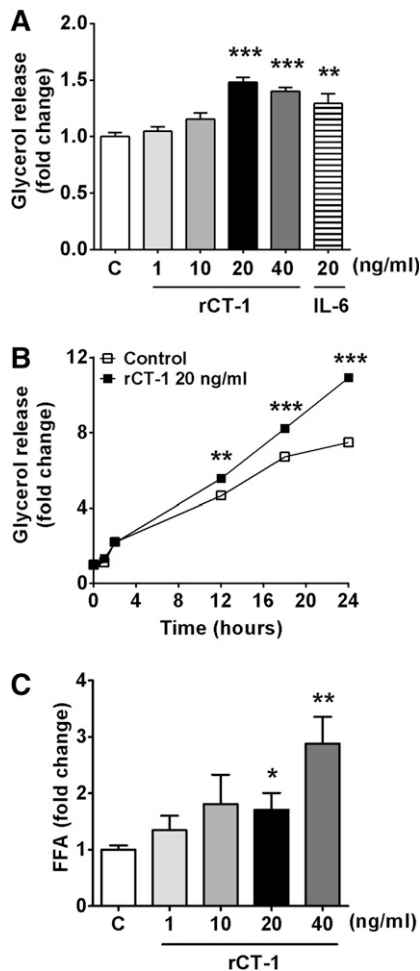


**Fig. 1.** CT-1 induces lipolysis in differentiated 3T3-L1 adipocytes. **A:** Fully differentiated 3T3-L1 adipocytes were serum starved for 4 h and then treated with various concentrations of rCT-1 (1, 10, 20, and 40 ng/ml) or IL-6 (20 ng/ml) for 18 h, and the amount of glycerol released into the media was measured. **B:** Time-response effects of rCT-1 (20 ng/ml) treatment on glycerol release. **C:** Dose-dependent effects of rCT-1 on FFAs release in adipocytes after 3 h of treatment. Data are mean  $\pm$  SEM ( $n = 5-7$ ). \* $P < 0.05$ , \*\* $P < 0.01$ , \*\*\* $P < 0.001$  compared with control (C) group.

a significant ( $P < 0.05$ ) decrease in ATGL protein levels (Fig. 2A, B). ATGL activity is regulated by CGI-58 (activator) and G0S2 (inhibitor) via noncompeting mechanisms (6). Our data provided evidence that in parallel with the inhibition of ATGL, rCT-1 treatment increased the content of the ATGL inhibitor G0S2 ( $P < 0.05$ ) after 24 h of treatment (Fig. 2A, D), while it did not significantly modify CGI-58 levels (Fig. 2A, C).

We next evaluated the effects of rCT-1 on HSL, a key lipase regulated by reversible phosphorylation (9). Our data revealed that rCT-1 (20 ng/ml) treatment increased the phosphorylation of HSL at Ser660 (which promotes its lipolytic activity), being significant after 2 ( $P < 0.05$ ) and 24 h ( $P < 0.05$ ) of treatment. However, rCT-1 did not modify the phosphorylation of HSL at Ser563 or Ser565 (Fig. 3A). To better characterize the involvement of HSL activation in the lipolytic actions of rCT-1, we tested the effect of the cytokine in HSL depleted adipocytes using siRNA. Our

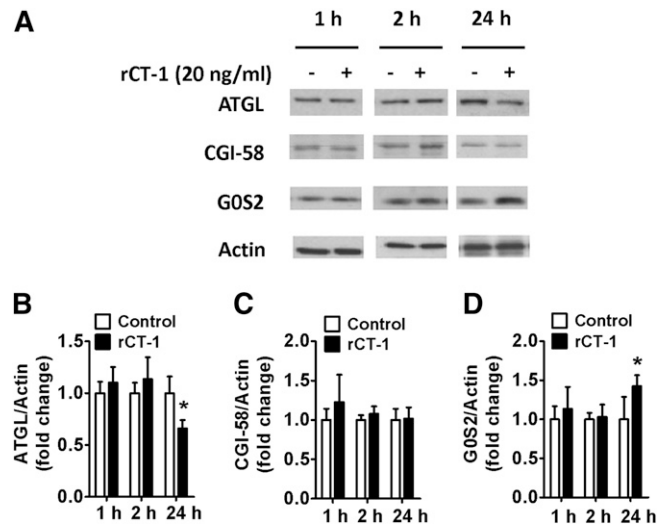


**Fig. 2.** ATGL is downregulated after 24 h of rCT-1 treatment. **A:** Representative Western blot and (B–D) densitometric analysis of ATGL (B), CGI-58 activator of ATGL (C), and G0S2 inhibitor of ATGL (D) in differentiated 3T3-L1 adipocytes treated with rCT-1 (20 ng/ml) or vehicle (Control) for 24 h. Band intensities for ATGL, CGI-58, and G0S2 were normalized to actin. Data are expressed as mean  $\pm$  SEM ( $n = 4-7$ ). \* $P < 0.05$  compared with vehicle-treated cells.

data revealed that rCT-1-induced glycerol release was almost completely abolished after silencing of HSL expression in adipocytes (Fig. 3B).

Finally, we also analyzed the effects of rCT-1 on perilipin A, an essential lipid droplet-associated protein, whose phosphorylation (PKA-dependent) is essential for the translocation of HSL from the cytosol to the lipid droplet surface (19). Using a perilipin-specific antibody and a phospho-PKA-motif-specific substrate antibody (15, 20), our data showed that rCT-1 caused a significant increase ( $P < 0.05$ ) in the phospho-PKA substrate/perilipin ratio after 24 h of treatment (Fig. 3C), suggesting the involvement of PKA activation in the lipolytic actions of CT-1 in cultured adipocytes.

#### Characterization of the signaling pathways involved in the lipolytic actions of CT-1

Several signaling pathways have been found to be involved in the regulation of lipolysis, including cAMP/PKA, AMPK, and cyclic guanosine monophosphate (cGMP)-dependent protein kinase-I by different lipolytic/antilipolytic agents (21). Our data demonstrated that lipolytic actions of rCT-1 were completely reversed ( $P < 0.001$ ) by pretreatment with the PKA inhibitor H89 (Fig. 4A). Moreover, the blocking of PKA also reversed rCT-1-induced phosphorylation of perilipin and HSL at Ser660 ( $P < 0.001$ ) (Fig. 4B). The involvement of PKA in the lipolytic action of rCT-1 was further supported by the fact that silencing of PKA expression using siRNA dramatically decreases rCT-1-stimulated glycerol release in adipocytes (Fig. 4C). Because these data suggest that CT-1 lipolytic actions take place by activation of the cAMP/PKA pathway, we also tested the effects of rCT-1 on cAMP, showing a significant ( $P < 0.01$ ) increase in cAMP levels in rCT-1-treated

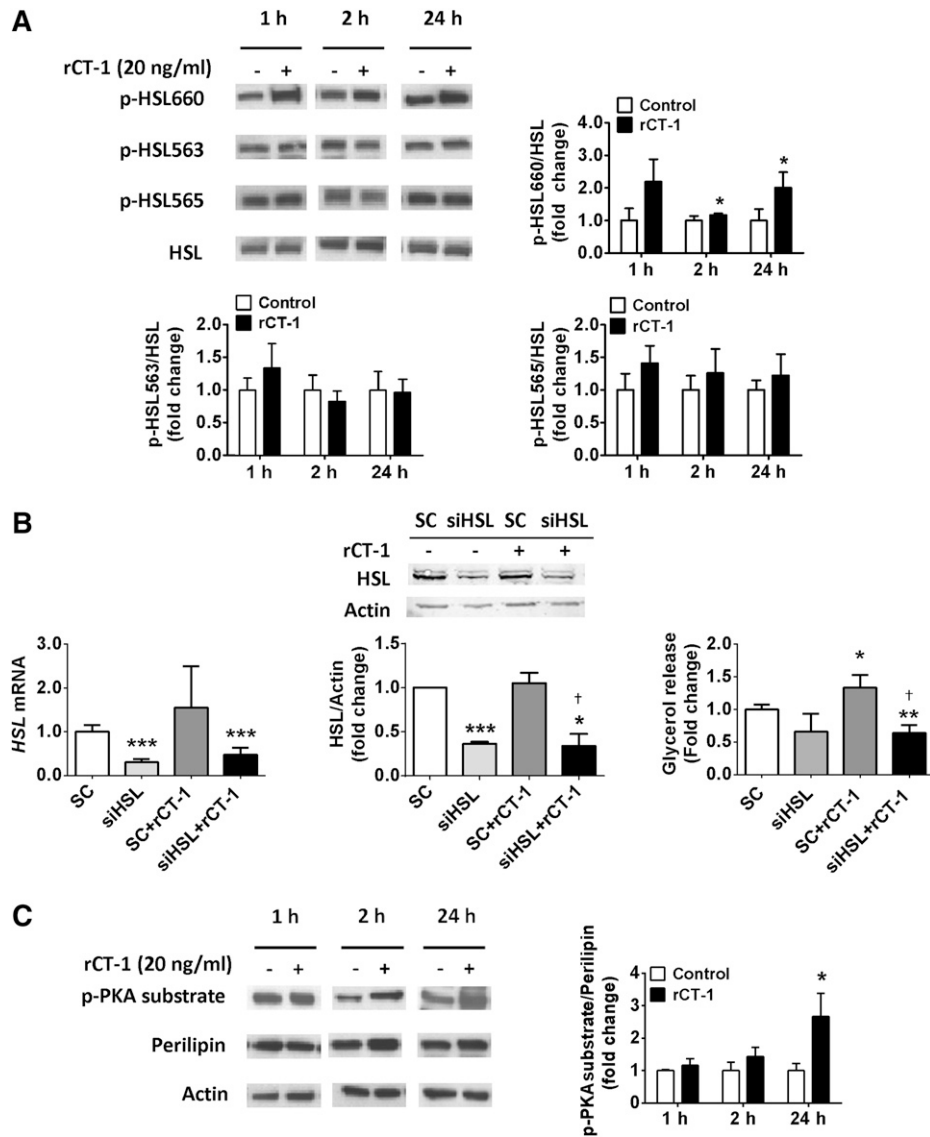


**Fig. 3.** HSL is involved in rCT-1-induced lipolysis. **A:** Representative Western blot and densitometric analysis of HSL phosphorylation at Ser660, Ser563, and Ser565 in differentiated 3T3-L1 adipocytes normalized by total HSL protein. **B:** rCT-1-stimulated lipolysis is prevented by siRNA knock-down of HSL. mRNA levels, protein expression of HSL, and glycerol release in 3T3-L1 adipocytes transfected with control siRNA (SC) or siRNA targeting endogenous HSL in the presence or absence of rCT-1 for 24 h. **C:** Adipocyte lysates were immunoblotted using a phospho-PKA-motif-specific antibody, and the blots were stripped and reblotted with antiperilipin antibodies to detect native perilipins. Band density was quantified, and data were expressed as phospho-PKA (p-PKA) substrate/perilipin ratio. Results are expressed as mean  $\pm$  SEM. ( $n = 4-7$ ). \* $P < 0.05$ , \*\* $P < 0.01$ , \*\*\* $P < 0.001$  versus control (vehicle-treated cells); † $P < 0.05$  compared with CT-1-treated cells.

adipocytes (**Fig. 5A**). In order to elucidate the mechanisms by which rCT-1 increases cAMP levels in adipocytes, we tested the effects of the cytokine on G protein-receptor complexes regulating adenylate cyclase. As shown in **Fig. 5B**, treatment with rCT-1 induced a significant increase in protein expression of  $G_{\alpha s}$ , a protein which couples stimulatory receptors to adenylyl cyclase, whereas no changes were observed in  $G_i$  protein, which inhibits adenylyl cyclase. Moreover, neither the levels of phospho-PDE3B nor the levels of AdPLA were modified by rCT-1 (supplementary **Fig. IIA, B**).

Treatment with the AMPK activator, AICAR, was also able to prevent the stimulation of glycerol release ( $P < 0.001$ ),

as well as the phosphorylation of Ser660 HSL ( $P < 0.05$ ) and perilipin ( $P < 0.01$ ) (**Fig. 4A, B**). On the other hand, pretreatment with PKG inhibitor KT5823 did not modify the stimulatory action of rCT-1 on glycerol release (**Fig. 4A**) or the phosphorylation of HSL and perilipin (**Fig. 4B**).

#### In vivo effects of rCT-1 treatment on HSL, perilipin, ATGL, CGI-58, and G0S2 in adipose tissue of mice

Finally, we aimed to analyze whether the effects of rCT-1 on lipolysis observed in cultured adipocytes were also reproduced in adipose tissue after in vivo administration of the cytokine in mice. Interestingly, we found that rCT-1

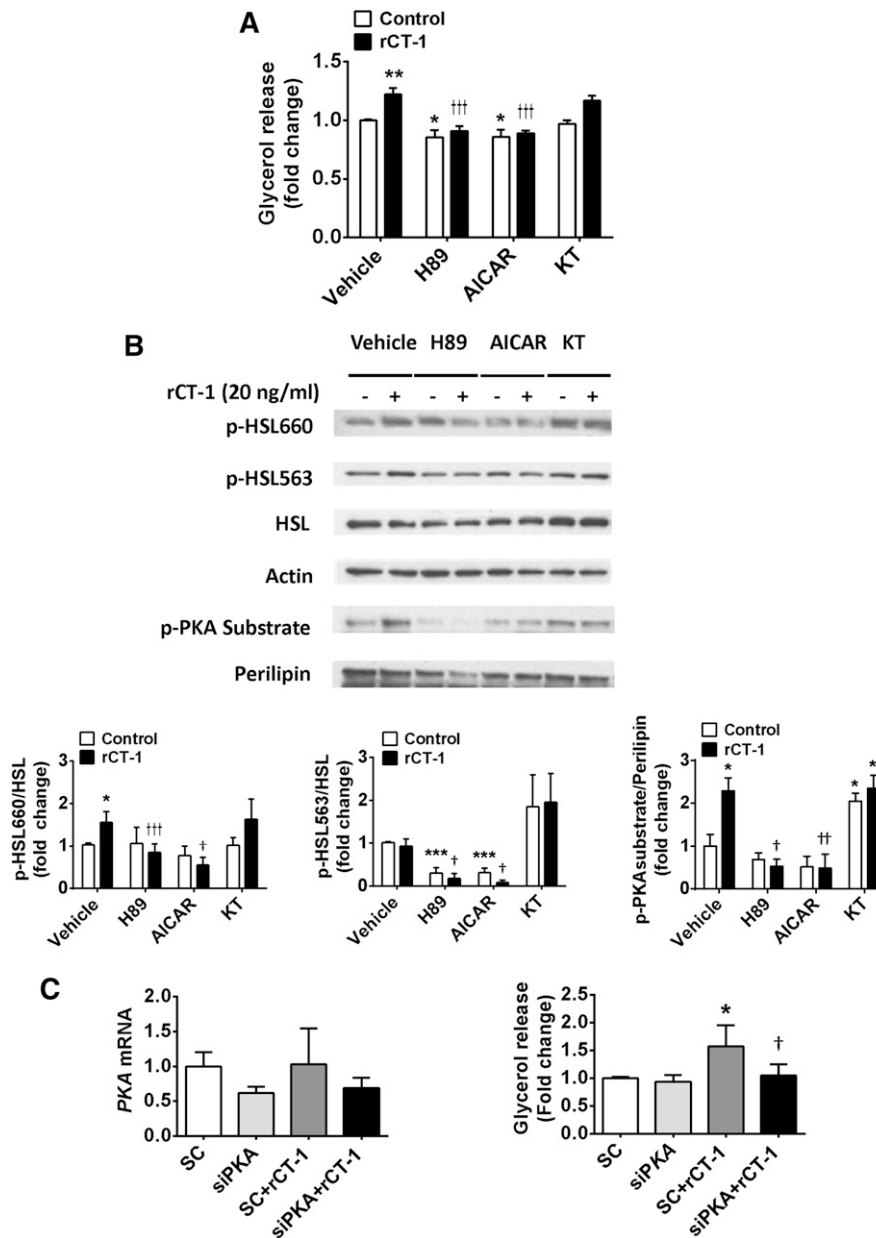


**Fig. 4.** PKA signaling pathway is involved in the lipolytic action of rCT-1. **A:** Effects of rCT-1 (20 ng/ml) treatment on glycerol release in differentiated 3T3-L1 adipocytes pretreated for 1 h in the presence or absence of PKA inhibitor H89 (1  $\mu$ M), AMPK activator AICAR (2 mM), and PKG inhibitor KT5823 (1  $\mu$ M), and then exposed to rCT-1 (20 ng/ml) or vehicle (DMSO) for 24 h. **B:** Representative Western blot and densitometric analysis of phospho-HSL660 (p-HSL660), phospho-HSL563 (p-HSL563) normalized by total HSL protein, and phospho-PKA (p-PKA) substrate/perilipin ratio. **C:** rCT-1-stimulated lipolysis is prevented by siRNA knock-down of PKA. mRNA levels of PKA and glycerol release in samples transfected with control siRNA (SC) or siPKA in either the absence or presence of rCT-1 for 24 h. Data are expressed as mean  $\pm$  SEM ( $n = 3-7$ ). \* $P < 0.05$ , \*\* $P < 0.01$ , \*\*\* $P < 0.001$  compared with control (vehicle-treated cells); † $P < 0.05$ , †† $P < 0.01$ , ††† $P < 0.001$  compared with rCT-1-treated cells.

treatment (0.2 mg/kg) for 30 min induced a significant increase in HSL phosphorylation at both Ser660 ( $P < 0.05$ ) and Ser563 ( $P < 0.001$ ) as compared with control mice. However, AMPK-mediated phosphorylation of HSL on Ser565, which prevents HSL activation, was significantly ( $P < 0.001$ ) decreased. Moreover, rCT-1 treatment boosted ( $P < 0.05$ ) PKA-mediated phosphorylation of perilipin (Fig. 6A). These results further support the key role of the

PKA pathway in the lipolytic action of CT-1. A statistically significant increase ( $P < 0.05$ ) in ATGL protein levels was also found in epididymal fat of *ob/ob* mice after 30 min of rCT-1 treatment, whereas neither the activator (CGI-58), nor the inhibitor (G0S2) of ATGL activity showed any changes after rCT-1 treatment (Fig. 6B). These facts suggest the ability of rCT-1 to promote lipolysis in vivo. In support of this, we found that the administration of rCT-1

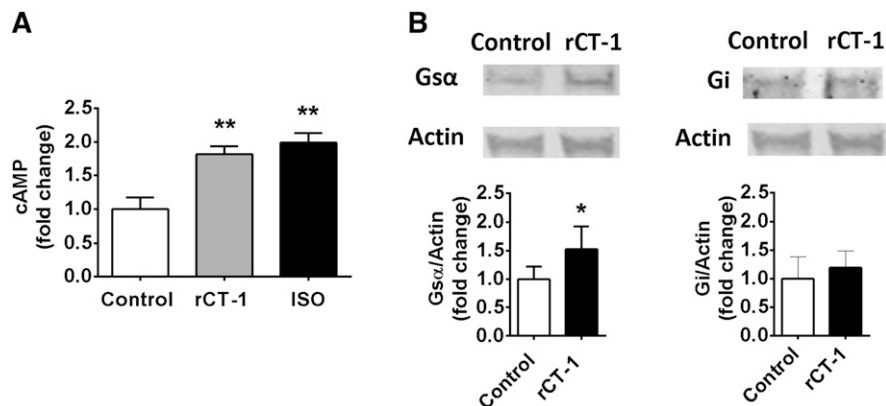


**Fig. 5.** rCT-1 stimulates  $G_{\alpha}$  and cAMP levels. A: Intracellular cAMP levels after 24 h of treatment with rCT-1 (20 ng/ml). B: Representative Western blot and densitometric analysis of  $G_{\alpha}$  and Gi protein levels in rCT-1-treated 3T3-L1 adipocytes. Data are expressed as mean  $\pm$  SEM ( $n = 4-7$ ). \* $P < 0.05$ , \*\* $P < 0.01$  compared with control (vehicle-treated cells).

(0.2 mg/kg) for 30 min to lean mice caused an increase in the levels of plasma FFAs in comparison with saline-treated mice (supplementary Fig. IIIA). Moreover, adipose tissue explants from rCT-1-treated mice exhibited increased lipolytic response as compared with the vehicle-treated group (supplementary Fig. IIIB).

## DISCUSSION

The present study demonstrates the lipolytic activity of CT-1 in adipocytes both in vitro and in vivo. In fact, in cultured adipocytes, CT-1 treatment promoted a decrease in intracellular TAG in parallel with an increase in the release of glycerol and FFAs, suggesting the ability of CT-1 to promote TAG catabolism. Interestingly, we found that CT-1 stimulates lipolysis in adipocytes through the regulation of the major lipases and lipid droplet proteins involved in the hydrolysis of TAG. Indeed, CT-1 promotes HSL phosphorylation at Ser660, a residue that is involved in the activation of this lipase. It is well-known that PKA is the major kinase involved in the phosphorylation of HSL at the sites that cause HSL activation, including Ser563, Ser659, and Ser660. However, in the present study we observed that CT-1 selectively induces the phosphorylation of Ser660 without affecting Ser563 in cultured adipocytes. In this context, it has been described that phosphorylation sites Ser659 and Ser660 are the critical activity controlling sites, whereas Ser563 plays a minor role in direct activation of HSL in vitro (11). Importantly, activation of HSL seems to be a key factor for the lipolytic action of CT-1, because silencing of HSL expression in adipocytes completely abolished CT-1-induced glycerol release, and partly prevented basal lipolysis.

Nevertheless, our in vivo studies revealed that acute administration of CT-1 to mice was able to stimulate adipose tissue lipolysis and to phosphorylate HSL, not only at Ser660, but also a dramatic stimulation at Ser563 was observed. It is important to take into account that in vivo, the regulation of PKA-stimulated HSL Ser563 and Ser660 phosphorylation seems to be time- and tissue-dependent.

In fact, a different time-response pattern for Ser563 and Ser660 phosphorylation has been described at diverse times during/after exercise in human adipose tissue. Moreover, a differential response in HSL phosphorylation was observed for Ser563 and Ser660 after treatment with  $\beta$ -adrenergic and AMPK stimulation in 3T3-L1 adipocytes (9). These facts suggest that although PKA is able to stimulate the phosphorylation of both Ser residues of HSL, the magnitude and time-response pattern could be different.

Other findings also support the view that the CT-1-induced lipolysis is secondary to the activation of the cAMP/PKA pathway: *i*) CT-1 increases cAMP intracellular content; *ii*) CT-1 promotes PKA-mediated phosphorylation of perilipin, enabling the translocation of phosphorylated HSL from the cytoplasm to the lipid droplet surface (22); *iii*) the PKA inhibitor, H89, blunts the phosphorylation of the two main PKA-targets, perilipin and HSL (at Ser660), and the subsequent increase in glycerol release induced by CT-1; and *iv*) silencing of PKA expression in adipocytes almost completely abrogated CT-1-induced glycerol release. Increased cAMP levels could be the consequence of increased adenylyl cyclase activity or reduced cAMP degradation (mainly mediated by PDE3B action). It is well-established that the stimulation of  $G_s$ -coupled receptors induces the activation of adenylyl cyclase, leading to increased intracellular cAMP levels and subsequent activation of PKA and phosphorylation and translocation of HSL to fat droplets (23, 24). Here, we demonstrate that CT-1 increased the levels of  $G_{\alpha}$  without affecting Gi, the inhibitory protein of adenylyl cyclase. Our findings also revealed that neither the levels of PDE3B, an enzyme that catalyses the breakdown of cAMP to its inactive form, nor the levels of AdPLA, which inhibits cAMP production by regulating prostaglandin  $E_2$  abundance, were modified by CT-1. Taken together, these findings suggest that CT-1-induced increase of cAMP is secondary to stimulatory guanine nucleotide binding protein ( $G_s$ )-mediated stimulation of adenylyl cyclase. CT-1 exerts its signaling effects by interacting with the gp130 receptor. This receptor shares a large degree of sequence homology with the leptin receptor, and both activate the Janus kinase/signal transducer and



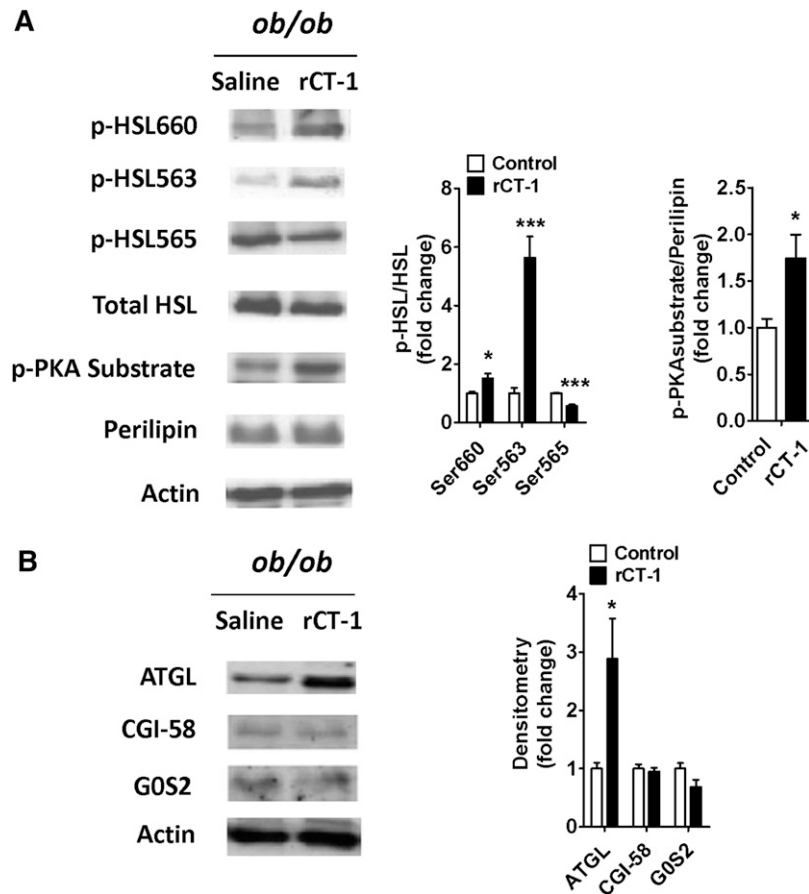


**Fig. 6.** In vivo administration of rCT-1 (0.2 mg/kg of body weight) for 30 min stimulates the main lipolytic enzymes in adipose tissue of *ob/ob* mice. A: Representative Western blot and densitometric analysis of HSL phosphorylation (Ser563, Ser660, Ser565) and perilipin in epididymal fat. Phospho-HSL (p-HSL) band intensities were normalized to total HSL, and phospho-PKA (p-PKA) substrate bands were normalized to perilipin. B: Representative Western blot and densitometric analysis of ATGL, CGI-58, and G0S2 in epididymal fat from *ob/ob* mice treated with rCT-1 or vehicle. Band intensities for ATGL, CGI-58, and G0S2 were normalized to actin. Results are expressed as mean  $\pm$  SEM (n = 4–7). \* $P < 0.05$ , \*\*\* $P < 0.001$ .

activator of transcription (JAK/STAT) and ERK signaling pathways (25). However, the lipolytic effect of leptin has been related to the downregulation of the adenylyl cyclase-inhibitory G protein pathway (26). In this context, growing evidence exists for a cross-talk of signaling cascades initiated by G protein-coupled receptors (GPCRs) and the IL-6 family of cytokines signaling pathway (27). In contrast to CT-1, TNF- $\alpha$  stimulates lipolysis in adipocytes by decreasing  $G_i$  without affecting  $G_s$  levels (28) or by downregulating the expression of PDE3B (29).

Our present data indicate that besides the stimulatory effect of CT-1 on lipolysis, ATGL protein levels are inhibited in long-term (24 h) CT-1-treated cultured adipocytes, in parallel with the increase of the ATGL inhibitor, G0S2 (30). This apparently surprising finding of downregulation of ATGL together with increased lipolysis has been described after treatment with some lipolytic molecules, such as TNF- $\alpha$ , in cultured adipocytes (31, 32). This may suggest that an interaction between these two regulatory processes (activity and expression) occurs (high ATGL activity might be compensated by low expression) (33). Similarly to HSL, ATGL activity is also stimulated by cate-

cholamines, but in contrast to HSL, ATGL activity is not directly regulated posttranslationally via PKA-mediated phosphorylation (34). It is well-known that ATGL protein is mainly coactivated by CGI-58 and inhibited by G0S2. However, the transcriptional regulation of ATGL is poorly characterized. In this context, PPAR $\gamma$  has been identified as a regulator of ATGL levels (34). It has been described that CT-1 induces a transient decrease in PPAR $\gamma$  in adipocytes at 24 h (3). In concordance, our data revealed that the decrease in ATGL observed after 24 h of treatment with CT-1 in cultured adipocytes paralleled with the drop in PPAR $\gamma$  levels (data not shown), suggesting a potential association between both events. In contrast with the lack of effect of short-term treatments (1–2 h) with CT-1 on ATGL in cultured adipocytes, the in vivo acute administration of CT-1 induced a marked increase in ATGL protein levels at 30 min, suggesting that putatively some mechanisms may regulate ATGL protein expression in vivo that do not exist in the in vitro model. In this context, several studies of our group have revealed that acute administration of CT-1 to mice has profound peripheral and central effects acting on neurohormonal regulators that could



also secondarily affect adipose tissue lipolysis. Thus, CT-1 stimulates insulin signaling and sensitivity, decreases blood glucose, activates AMPK and promotes fatty acid oxidation in muscle and liver, and modulates hypothalamic pathways involved in energy intake (4, 35). Interestingly, growing evidence suggests a role of hypothalamic regulation of adipose tissue function and metabolism (36).


AMPK has also been shown as an important regulator of lipolysis by regulating both HSL and ATGL activity by phosphorylation. Nevertheless, the effects of AMPK activation on lipolysis are complex because both antilipolytic (37–39) and lipolytic (40, 41) actions have been reported. In fact, AMPK effects on lipolysis seem to be time-dependent, involving antagonistic modulation of HSL and ATGL (42). In this context, several trials have demonstrated that AMPK induces phosphorylation of HSL at Ser565, which prevents phosphorylation of HSL by cyclic AMP-dependent protein kinase (PKA), causing suppression of PKA-stimulated lipolysis (43). On the other hand, AMPK phosphorylates ATGL at Ser406, increasing TAG hydrolase activity and providing evidence for increased lipolysis (8). The present data show that AMPK activation totally abolishes the lipolytic effect of CT-1 and suggest that AICAR-induced phosphorylation of HSL at Ser565 is able to prevent CT-1 induced-PKA-mediated phosphorylation and activation of HSL.

Activation of the cGMP pathway has also been shown to promote lipolysis. A downstream effector of cGMP, cGMP-dependent protein kinase, also called PKG, was shown to induce perilipin and HSL phosphorylation and to be at the origin of atrial natriuretic peptide-induced lipolysis (44). We tested the potential involvement of the cGMP/PKG pathway in the lipolytic actions of CT-1. The results suggest that this pathway is not involved in CT-1-stimulated lipolysis because treatment with the PKG inhibitor, KT5823, was not able to reverse CT-1-induced glycerol release and did not cause any significant changes in HSL or perilipin activation.

Several studies have described lipolytic actions in adipocytes for IL-6 (45) and other members of the gp130 ligand family of cytokines such as leukemia inhibitory factor (46). However, differential effects have been found among cytokines of this family. For example, previous studies by our group have shown that chronic administration of CT-1 to obese mice stimulated the lipolytic response to isoproterenol in adipocytes (4). On the other hand, no significant changes in lipolysis were found after the administration of ciliary neurotrophic factor to high-fat-fed mice (47). The study by Wolsk et al. (48) showed that an acute increase in IL-6 selectively stimulates lipolysis in skeletal muscle, whereas adipose tissue was unaffected in humans. Our present study clearly shows an increase of the main lipases in adipose tissue after an acute administration of CT-1. Additional findings also suggest differential mechanisms of action underlying the lipolytic properties of CT-1 and IL-6. Thus, it has been observed that IL-6 increased lipolysis in differentiated porcine adipocytes by activation of ERK, which was inhibited by a specific ERK inhibitor, while IL-6 treatment did not elevate intracellular cAMP, and the specific PKA inhibitor (H89) did not affect IL-6-induced

lipolysis, suggesting that the PKA pathway was not involved in IL-6 lipolytic effects (49). On the contrary, our present data clearly suggest the involvement of the cAMP/PKA pathway in the lipolytic action of CT-1.

Activation of lipolysis has been proposed as a promising therapeutic target for the treatment of obesity (50). Our results suggest that the ability of CT-1 to activate the pathway in adipocytes could also contribute to its anti-obesity properties. In line with this, we have previously reported that chronic administration of CT-1 to *ob/ob* mice increased the adipocytes' lipolytic response to isoproterenol (4). It is important to mention that increased lipolysis and FFAs release from adipose tissue have been associated with the development of metabolic disturbances in obesity (51). However, several studies have suggested that increasing lipolysis in adipose tissue does not necessarily increase serum FFAs levels, because increasing lipolysis in adipose tissue causes a shift within adipocytes toward increased FFAs utilization and energy expenditure and, thus, protects against obesity (50). In this context, our previous data revealed that CT-1 is able to promote FFAs oxidation not only in adipose tissue but also in muscle, reducing insulin resistance in obese mice (4).

In summary, the present data demonstrate that the ability of CT-1 to regulate the activity of the main lipases underlies the lipolytic action of this cytokine *in vitro* and *in vivo*, and may account for the anti-obesity effects of CT-1. 

## REFERENCES

1. Pennica, D., K. J. Shaw, T. A. Swanson, M. W. Moore, D. L. Shelton, K. A. Zioncheck, A. Rosenthal, T. Taga, N. F. Paoni, and W. I. Wood. 1995. Cardiotrophin-1. Biological activities and binding to the leukemia inhibitory factor receptor/gp130 signaling complex. *J. Biol. Chem.* **270**: 10915–10922.
2. Natal, C., M. A. Fortunato, P. Restituto, A. Bazan, I. Colina, J. Diez, and N. Varo. 2008. Cardiotrophin-1 is expressed in adipose tissue and upregulated in the metabolic syndrome. *Am. J. Physiol. Endocrinol. Metab.* **294**: E52–E60.
3. Zvonic, S., J. C. Hogan, P. Arbour-Reily, R. L. Mynatt, and J. M. Stephens. 2004. Effects of cardiotrophin on adipocytes. *J. Biol. Chem.* **279**: 47572–47579.
4. Moreno-Aliaga, M. J., N. Perez-Echarri, B. Marcos-Gomez, E. Larequi, F. J. Gil-Bea, B. Viollet, I. Gimenez, J. A. Martinez, J. Prieto, and M. Bustos. 2011. Cardiotrophin-1 is a key regulator of glucose and lipid metabolism. *Cell Metab.* **14**: 242–253.
5. Zimmermann, R., J. G. Strauss, G. Haemmerle, G. Schoiswohl, R. Birner-Gruenberger, M. Riederer, A. Lass, G. Neuberger, F. Eisenhaber, A. Hermetter, et al. 2004. Fat mobilization in adipose tissue is promoted by adipose triglyceride lipase. *Science*. **306**: 1383–1386.
6. Lu, X., X. Yang, and J. Liu. 2010. Differential control of ATGL-mediated lipid droplet degradation by CGI-58 and G0S2. *Cell Cycle*. **9**: 2719–2725.
7. Cornaciu, I., A. Boeszoermyeni, H. Lindermuth, H. M. Nagy, I. K. Cerk, C. Ebner, B. Salzbürger, A. Gruber, M. Schweiger, J. Zechner, et al. 2011. The minimal domain of adipose triglyceride lipase (ATGL) ranges until leucine 254 and can be activated and inhibited by CGI-58 and G0S2, respectively. *PLoS ONE*. **6**: e26349.
8. Ahmadian, M., M. J. Abbott, T. Tang, C. S. Hudak, Y. Kim, M. Bruss, M. K. Hellerstein, H. Y. Lee, V. T. Samuel, G. I. Shulman, et al. 2011. Desnutrin/ATGL is regulated by AMPK and is required for a brown adipose phenotype. *Cell Metab.* **13**: 739–748.
9. Watt, M. J., A. G. Holmes, S. K. Pinnamaneni, A. P. Garnham, G. R. Steinberg, B. E. Kemp, and M. A. Febbraio. 2006. Regulation of

- HSL serine phosphorylation in skeletal muscle and adipose tissue. *Am. J. Physiol. Endocrinol. Metab.* **290**: E500–E508.
10. Greenberg, A. S., W. J. Shen, K. Muliro, S. Patel, S. C. Souza, R. A. Roth, and F. B. Kraemer. 2001. Stimulation of lipolysis and hormone-sensitive lipase via the extracellular signal-regulated kinase pathway. *J. Biol. Chem.* **276**: 45456–45461.
  11. Anthonen, M. W., L. Ronnstrand, C. Wernstedt, E. Degerman, and C. Holm. 1998. Identification of novel phosphorylation sites in hormone-sensitive lipase that are phosphorylated in response to isoproterenol and govern activation properties in vitro. *J. Biol. Chem.* **273**: 215–221.
  12. Brasaemle, D. L. 2007. Adipocyte biology. The perilipin family of structural lipid droplet proteins: stabilization of lipid droplets and control of lipolysis. *J. Lipid Res.* **48**: 2547–2559.
  13. Granneman, J. G., H. P. Moore, R. Krishnamoorthy, and M. Rathod. 2009. Perilipin controls lipolysis by regulating the interactions of AB-hydrolase containing 5 (Abhd5) and adipose triglyceride lipase (Atgl). *J. Biol. Chem.* **284**: 34538–34544.
  14. Miyoshi, H., J. W. Perfield 2nd, S. C. Souza, W. J. Shen, H. H. Zhang, Z. S. Stancheva, F. B. Kraemer, M. S. Obin, and A. S. Greenberg. 2007. Control of adipose triglyceride lipase action by serine 517 of perilipin A globally regulates protein kinase A-stimulated lipolysis in adipocytes. *J. Biol. Chem.* **282**: 996–1002.
  15. Fernández-Galilea, M., P. Pérez-Matute, P. L. Prieto-Hontoria, J. A. Martínez, and M. J. Moreno-Aliaga. 2012. Effects of lipoic acid on lipolysis in 3T3-L1 adipocytes. *J. Lipid Res.* **53**: 2296–2306.
  16. Beraza, N., J. M. Marques, E. Martínez-Anso, M. Iniguez, J. Prieto, and M. Bustos. 2005. Interplay among cardiostrophin-1, prostaglandins, and vascular endothelial growth factor in rat liver regeneration. *Hepatology*. **41**: 460–469.
  17. Takahashi, Y., A. Shinoda, N. Furuya, E. Harada, N. Arimura, I. Ichi, Y. Fujiwara, J. Inoue, and R. Sato. 2013. Perilipin-mediated lipid droplet formation in adipocytes promotes sterol regulatory element-binding protein-1 processing and triacylglyceride accumulation. *PLoS ONE*. **8**: e64605.
  18. Yeaman, S. J. 2004. Hormone-sensitive lipase—new roles for an old enzyme. *Biochem. J.* **379**: 11–22.
  19. Sztalryd, C., G. Xu, H. Dorward, J. T. Tansey, J. A. Contreras, A. R. Kimmel, and C. Londos. 2003. Perilipin A is essential for the translocation of hormone-sensitive lipase during lipolytic activation. *J. Cell Biol.* **161**: 1093–1103.
  20. Choi, S. M., D. F. Tucker, D. N. Gross, R. M. Easton, L. M. DiPilato, A. S. Dean, B. R. Monk, and M. J. Birnbaum. 2010. Insulin regulates adipocyte lipolysis via an Akt-independent signaling pathway. *Mol. Cell. Biol.* **30**: 5009–5020.
  21. Nishikimi, T., C. Iemura-Inaba, K. Akimoto, K. Ishikawa, S. Koshikawa, and H. Matsuoka. 2009. Stimulatory and inhibitory regulation of lipolysis by the NPR-A/cGMP/PKG and NPR-C/G(i) pathways in rat cultured adipocytes. *Regul. Pept.* **153**: 56–63.
  22. Brasaemle, D. L., D. M. Levin, D. C. Adler-Wailles, and C. Londos. 2000. The lipolytic stimulation of 3T3-L1 adipocytes promotes the translocation of hormone-sensitive lipase to the surfaces of lipid storage droplets. *Biochim. Biophys. Acta.* **1483**: 251–262.
  23. Belfrage, P., G. Fredrikson, N. O. Nilsson, and P. Stralfors. 1981. Regulation of adipose-tissue lipolysis by phosphorylation of hormone-sensitive lipase. *Int. J. Obes.* **5**: 635–641.
  24. Chaves, V. E., D. Frasson, and N. H. Kawashita. 2011. Several agents and pathways regulate lipolysis in adipocytes. *Biochimie*. **93**: 1631–1640.
  25. Febbraio, M. A. 2007. gp130 receptor ligands as potential therapeutic targets for obesity. *J. Clin. Invest.* **117**: 841–849.
  26. Frühbeck, G., L. Méndez-Giménez, J. A. Fernández-Formoso, S. Fernández, and A. Rodríguez. 2014. Regulation of adipocyte lipolysis. *Nutr. Res. Rev.* **27**: 63–93.
  27. Garbers, C., H. M. Hermanns, F. Schaper, G. Muller-Newen, J. Grotzinger, S. Rose-John, and J. Scheller. 2012. Plasticity and cross-talk of interleukin 6-type cytokines. *Cytokine Growth Factor Rev.* **23**: 85–97.
  28. Gasic, S., B. Tian, and A. Green. 1999. Tumor necrosis factor alpha stimulates lipolysis in adipocytes by decreasing Gi protein concentrations. *J. Biol. Chem.* **274**: 6770–6775.
  29. Rahn Landström, T., J. Mei, M. Karlsson, V. Manganiello, and E. Degerman. 2000. Down-regulation of cyclic-nucleotide phosphodiesterase 3B in 3T3-L1 adipocytes induced by tumor necrosis factor alpha and cAMP. *Biochem. J.* **346**: 337–343.
  30. Yang, X., X. Lu, M. Lombes, G. B. Rha, Y. I. Chi, T. M. Guerin, E. J. Smart, and J. Liu. 2010. The G(0)/G(1) switch gene 2 regulates adipose lipolysis through association with adipose triglyceride lipase. *Cell Metab.* **11**: 194–205.
  31. Lorente-Cebrián, S., M. Bustos, A. Marti, M. Fernández-Galilea, J. A. Martínez, and M. J. Moreno-Aliaga. 2012. Eicosapentaenoic acid inhibits tumour necrosis factor-alpha-induced lipolysis in murine cultured adipocytes. *J. Nutr. Biochem.* **23**: 218–227.
  32. Kim, J. Y., K. Tillison, J. H. Lee, D. A. Rearick, and C. M. Smas. 2006. The adipose tissue triglyceride lipase ATGL/PNPLA2 is downregulated by insulin and TNF-alpha in 3T3-L1 adipocytes and is a target for transactivation by PPARgamma. *Am. J. Physiol. Endocrinol. Metab.* **291**: E115–E127.
  33. Kralisch, S., J. Klein, U. Lossner, M. Blüher, R. Paschke, M. Stumvoll, and M. Fasshauer. 2005. Isoproterenol, TNFalpha, and insulin downregulate adipose triglyceride lipase in 3T3-L1 adipocytes. *Mol. Cell. Endocrinol.* **240**: 43–49.
  34. Kershaw, E. E., M. Schupp, H. P. Guan, N. P. Gardner, M. A. Lazar, and J. S. Flier. 2007. PPARgamma regulates adipose triglyceride lipase in adipocytes in vitro and in vivo. *Am. J. Physiol. Endocrinol. Metab.* **293**: E1736–E1745.
  35. Castaño, D., E. Larequi, I. Belza, A. M. Astudillo, E. Martínez-Ansó, J. Balsinde, J. Argemi, T. Aragon, M. J. Moreno-Aliaga, J. Muntane, et al. 2014. Cardiostrophin-1 eliminates hepatic steatosis in obese mice by mechanisms involving AMPK activation. *J. Hepatol.* **60**: 1017–1025.
  36. Stefanidis, A., N. M. Wiedmann, E. S. Adler, and B. J. Oldfield. 2014. Hypothalamic control of adipose tissue. *Best Pract. Res. Clin. Endocrinol. Metab.* **28**: 685–701.
  37. Dagon, Y., Y. Avraham, and E. M. Berry. 2006. AMPK activation regulates apoptosis, adipogenesis, and lipolysis by eIF2alpha in adipocytes. *Biochem. Biophys. Res. Commun.* **340**: 43–47.
  38. Boon, H., M. Bosselaar, S. F. Praet, E. E. Blaak, W. H. Saris, A. J. Wagenmakers, S. L. McGee, C. J. Tack, P. Smits, M. Hargreaves, et al. 2008. Intravenous AICAR administration reduces hepatic glucose output and inhibits whole body lipolysis in type 2 diabetic patients. *Diabetologia*. **51**: 1893–1900.
  39. Anthony, N. M., M. P. Gaidhu, and R. B. Ceddia. 2009. Regulation of visceral and subcutaneous adipocyte lipolysis by acute AICAR-induced AMPK activation. *Obesity (Silver Spring)*. **17**: 1312–1317.
  40. Koh, H. J., M. F. Hirshman, H. He, Y. Li, Y. Manabe, J. A. Balschi, and L. J. Goodyear. 2007. Adrenaline is a critical mediator of acute exercise-induced AMP-activated protein kinase activation in adipocytes. *Biochem. J.* **403**: 473–481.
  41. Yamaguchi, S., H. Katahira, S. Ozawa, Y. Nakamichi, T. Tanaka, T. Shimoyama, K. Takahashi, K. Yoshimoto, M. O. Imaizumi, S. Nagamatsu, et al. 2005. Activators of AMP-activated protein kinase enhance GLUT4 translocation and its glucose transport activity in 3T3-L1 adipocytes. *Am. J. Physiol. Endocrinol. Metab.* **289**: E643–E649.
  42. Gaidhu, M. P., S. Fedic, N. M. Anthony, M. So, M. Mirpourian, R. L. Perry, and R. B. Ceddia. 2009. Prolonged AICAR-induced AMP-kinase activation promotes energy dissipation in white adipocytes: novel mechanisms integrating HSL and ATGL. *J. Lipid Res.* **50**: 704–715.
  43. Garton, A. J., and S. J. Yeaman. 1990. Identification and role of the basal phosphorylation site on hormone-sensitive lipase. *Eur. J. Biochem.* **191**: 245–250.
  44. Sengenès, C., C. Moro, J. Galitzky, M. Berlan, and M. Lafontan. 2005. Natriuretic peptides: a new lipolytic pathway in human fat cells [article in French]. *Med. Sci. (Paris)*. **21**: 61–65.
  45. Ji, C., X. Chen, C. Gao, L. Jiao, J. Wang, G. Xu, H. Fu, X. Guo, and Y. Zhao. 2011. IL-6 induces lipolysis and mitochondrial dysfunction, but does not affect insulin-mediated glucose transport in 3T3-L1 adipocytes. *J. Bioenerg. Biomembr.* **43**: 367–375.
  46. Marshall, M. K., W. Doerrler, K. R. Feingold, and C. Grunfeld. 1994. Leukemia inhibitory factor induces changes in lipid metabolism in cultured adipocytes. *Endocrinology*. **135**: 141–147.
  47. Crowe, S., S. M. Turpin, F. Ke, B. E. Kemp, and M. J. Watt. 2008. Metabolic remodeling in adipocytes promotes ciliary neurotrophic factor-mediated fat loss in obesity. *Endocrinology*. **149**: 2546–2556.
  48. Wolsk, E., H. Mygind, T. S. Grondahl, B. K. Pedersen, and G. van Hall. 2010. IL-6 selectively stimulates fat metabolism in human skeletal muscle. *Am. J. Physiol. Endocrinol. Metab.* **299**: E832–E840.
  49. Yang, Y., D. Ju, M. Zhang, and G. Yang. 2008. Interleukin-6 stimulates lipolysis in porcine adipocytes. *Endocrine*. **33**: 261–269.
  50. Ahmadian, M., R. E. Duncan, and H. S. Sul. 2009. The skinny on fat: lipolysis and fatty acid utilization in adipocytes. *Trends Endocrinol. Metab.* **20**: 424–428.
  51. Ormseth, M. J., L. L. Swift, S. Fazio, M. F. Linton, C. P. Chung, P. Raggi, Y. H. Rho, J. Solus, A. Oeser, A. Bian, et al. 2011. Free fatty acids are associated with insulin resistance but not coronary artery atherosclerosis in rheumatoid arthritis. *Atherosclerosis*. **219**: 869–874.